Langmuir

Article

pubs.acs.org/Langmuir

Quantitative Estimation of the Parameters for Self-Motion Driven by Difference in Surface Tension

Nobuhiko J. Suematsu,*[,†,‡] Tomohiro Sasaki,[§] Satoshi Nakata,[∥] and Hiroyuki Kitahata[§]

[†]Graduate School of Advanced Mathematical Sciences, Meiji University, 4-21-1 Nakano, Tokyo 164-8525, Japan

[‡]Meiji Institute of Advanced Study of Mathematical Sciences, Meiji University, 4-21-1 Nakano, Tokyo 164-8525, Japan

[§]Department of Physics, Graduate School of Science, Chiba University, 1-33 Yayoi-cho, Inage-ku, Chiba 263-8522, Japan

[∥]Graduate School of Science, Hiroshima University, 1-3-1 Kagamiyama, Higashi-Hiroshima 739-8526, Japan

Supporting Information

ABSTRACT: Quantitative information on the parameters associated with self-propelled objects would enhance the potential of this research field; for example, finding a realistic way to develop a functional self-propelled object and quantitative understanding of the mechanism of self-motion. We therefore estimated five main parameters, including the driving force, of a camphor boat as a simple self-propelled object that spontaneously moves on water due to difference in surface tension. The experimental results and mathematical model indicated that the camphor boat generated a driving force of 4.2 μN, which corresponds to a difference in surface tension of 1.1 mN m^{-1}. The methods used in this study are not restricted to evaluate the parameters of self-motion of a camphor boat, but can be applied to other self-propelled objects driven by difference in surface tension. Thus, our investigation provides a novel method to quantitatively estimate the parameters for self-propelled objects driven by the interfacial tension difference.

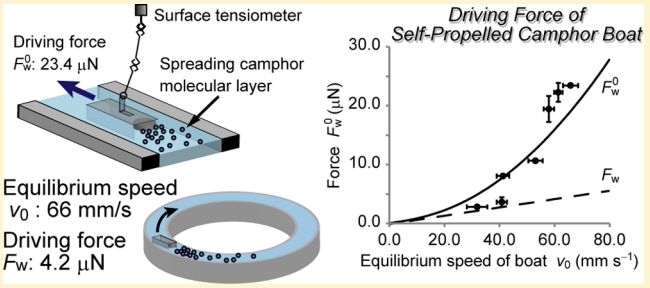

INTRODUCTION

A variety of inanimate self-propelled objects have been developed that can move spontaneously without any external driving forces, as is observed in living systems such as bacteria. Similar to living systems, most self-propelled objects isothermally transform chemical energy to kinetic energy using nonequilibrium conditions; this energy transformation mechanism is expected to be a promising technology for functional materials at the micrometer scale (e.g., searching systems that behave similar to chemotaxis or a mass transport system for such a drug delivery system or soft robotics).[1−3] Several driving mechanisms have been developed for self-propelled objects,[4] and one of the most popular mechanisms is based on interfacial tension gradient. For example, an object, such as a solid,[5] a liquid droplet,[6] or a gel,[7] is propelled on water or on a solid due to the difference in the interfacial tension around the object,[5−8] and small droplets spontaneously move within an oil or a water phase where an interfacial tension gradient is generated by a chemical reaction associated with the surfactants.[9−11]

An object driven by a difference in surface tension is one of the simplest self-propelled systems. The driving mechanism of these systems is caused by the difference in the interfacial tension around the object, which is generated by the dissolution of the surfactant from the object itself and pulls the object toward the higher-interfacial-tension region.[12] This simple mechanism has been verified qualitatively by numerous experiments and pertinent mathematical models.[13,14] On the basis of the qualitative understanding of the mechanism, researchers have investigated the addition of functionality to self-propelled objects through coupling with chemical structure, chemical reaction,[15] and a collection of the particles;[16,17] in addition, there have been reports suggesting possible theoretical approaches for evaluating such functional systems.[15−17] However, identifying suitable experimental conditions and feasibility assessment for such theoretical analyses is challenging. Thus, quantitative information about self-motion will strongly promote the realization of smart self-propelled objects.

In this paper, we describe a simple self-propelled camphor system that, for over a decade, has been used for the investigation of self-propelled objects.[18] The camphor system has advantages for a typical system as self-propelled objects because of a long lifetime of motion and large value on the driving force originated from rapid sublimation and dissolution and an easy designing of the shape.[12] We propose a methodology for determining the values of important parameters associated with the behavior of camphor molecules on water (e.g., the supply rate of camphor molecules from a solid disk to the surface of the water and the driving force of the camphor boat). Our results enable discussion of camphor

Received: April 28, 2014
Revised: June 4, 2014
Published: June 16, 2014

   dx.doi.org/10.1021/la501628d | Langmuir 2014, 30, 8101−8108

motion quantitatively. Furthermore, our novel methodology can apply to other systems and will estimate key parameters for other self-propelled objects driven by the interfacial tension difference.

EXPERIMENTAL SETUP

Two types of camphor boats were prepared: a round-shaped boat that exhibited self-motion with a circular trajectory and a rectangular-shaped boat that exhibited a straight trajectory. The former was used to measure the time series of the surface pressure and the latter to estimate other parameters, including the driving force of the camphor boat. Each boat was composed of a plastic plate (0.1 mm in thickness) and a camphor disk [3 mm in diameter (ϕ) and 1 mm in thickness]. The camphor disk was pressed using a pellet die set for the preparation of samples for Fourier transform-infrared (FT-IR) analysis. The round-shaped plastic boat (6 mm in diameter) was flat, and the camphor disk was attached at the edge of the plastic boat such that half of the disk was projected over the water (Figure 1a). The rectangular-shaped boat was made by bending both sides of a rectangular plastic plate (8 mm in width and 10 mm in height) at 2 mm from the edge, and thus the actual width of the boat (w) was 4 mm. The position of attachment of the camphor disk was defined by the distance (p) between the edge of boat and that of the camphor disk, as shown in Figure 1b. Basically, a boat with a distance p = 1.5 mm, in which half of the disk stuck out from the plastic plate, or p = −3.5 mm, in which the disk was attached at the center of the plate, was used for the measurements. When the driving force was measured, on the while, p varied from 0.0 to 1.5 mm.[19]

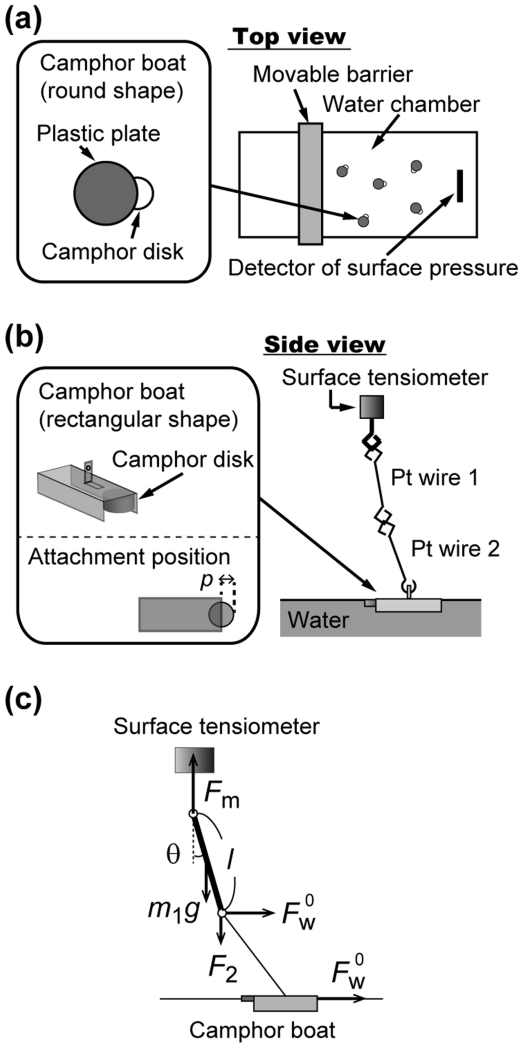

Figure 1. (a) Illustration of a round-shaped camphor boat and the experimental setup for measuring the time series of the surface pressure with self-propelled camphor boats. (b) Illustration of a rectangular-shaped camphor boat and the experimental setup for measuring the driving force of the camphor boat. (c) Force balance around Pt wire 1.

The time series of the surface pressure was measured to estimate the surface concentration of the camphor molecules. Five camphor boats were floated on the water phase in the chamber of a surface pressure meter (HMB-700LB, Kyowa Interface Science Co., Japan) with measuring the surface pressure (Figure 1a). The surface area of the water phase (A) was kept constant during the measurement (50−150 cm^2).

Camphor molecules spontaneously dissolved from the camphor disk toward the water phase, the air phase, and the water surface. The rates of these supplies were estimated by measuring the weight loss of camphor disks. At least three measurements were performed for each condition, and the results were averaged. First, to estimate the supply rate to the water phase, two camphor disks were dipped into water (60 mL of Milli-Q water in a 100 mL beaker) while stirring using a magnetic stirrer (300 rpm) for 2, 5, 10, 15, and 20 min. The total weight of the two camphor disks was measured before and after dipping, and the time series of the weight loss was obtained. To confirm that this method was practical, the weight loss was also measured using spectroscopy (Figure S1 of the Supporting Information). Next, five camphor disks were placed on a digital weight scale, and their weight loss was measured with respect to time. This measurement estimated the sublimation rate of camphor from one side of the disk. Finally, three camphor disks were floated on the surface of water (60 mL of Milli-Q water in a Petri dish of diameter 90 mm) for 2, 5, 10, 20, and 30 min. The total weight of the three camphor disks was measured before and after floating, and the weight loss was obtained for each floating time. When the disk was floated on the water surface, half of the camphor disk was dipped into the water phase, and the other side was exposed to the air phase. Thus, the rate of weight loss represents the sum of $\alpha_w/2 + \alpha_a + \alpha$, where α_w, α_a, and α are the supply rates for camphor molecules to the water phase, the air phase, and the water surface, respectively.

The spreading behavior of the camphor molecular layer on water was observed using visualizing particles ($CaSO_4$ powder). To prepare a camphor molecular layer, a camphor boat exhibiting intermittent motion (p = −3.5 mm) was gently floated on water. After a few tens of seconds, camphor molecules reached the edge of the boat and then rapidly spread.[19] Thereafter, the molecular layer swept up the visualizing particles. The time series of the size of the visualized molecular layer was observed using a digital video camera (Handycam HDR-CX180, Sony, Japan) operated at 30 frames per second, and the data were analyzed on a computer using an image analysis software (ImageJ, NIH).

The friction coefficient of the camphor boat was evaluated from the time series of its speed during the relaxation process. To observe the relaxation process, the intermittent motion of a camphor boat is suitable because such intermittent motion includes a relaxation-like process. Namely, the camphor boat rapidly accelerates and then gently decelerates due to friction. Thus, to obtain the time series, the intermittent motion of a camphor boat with the camphor disk attached at the center of a plastic boat (p = −3.5 mm)[19] was observed with a digital video camera. A total of 16 experiments were performed, and the results were averaged.

The driving force for the self-motion of a camphor boat was directly measured using a surface tensiometer (DY-300, Kyowa Interface Science Company, Japan). This method is hereafter referred to as the "direct mechanical measurement" method. A surface tensiometer measures the intensity of the force working on a detector. In this method, a rectangular-shaped camphor boat was connected to the detector using Pt wires (0.1 mm in diameter, 7 mg in mass, and 100 mm in length), as illustrated in Figure 1b. A Petri dish (150 mm in diameter and 5 mm of water depth) was used as the water chamber.

dx.doi.org/10.1021/la501628d | Langmuir 2014, 30, 8101−8108

The camphor boat connected to the detector was floated on water that was restricted to a narrow channel (6 mm in width) using silicone rubber sheets. After the boat stopped, which meant that the system reached a mechanical equilibrium condition, the force working on the detector (F_m) was measured using the surface tensiometer, and the tilt angle of the Pt wire 1 (θ) was observed by analyzing a photo using a computer. From the values for F_m and θ, the driving force of the stationary camphor boat (F_w^0) was estimated.

The camphor boat pulled the edge of the Pt wire and stopped at an equilibrium position where the mechanical forces were balanced. The force and torque balance conditions near Pt wire 1 are described as follows:

Force balance in the vertical direction:

$$F_m = m_1 g + F_2 \tag{1}$$

Torque balance:

$$\frac{1}{2} l m_1 g \sin\theta + l F_2 \sin\theta - l F_w^0 \cos\theta = 0 \tag{2}$$

where the parameters are denoted in Figure 1c. From eqs 1 and 2, the following equation is obtained:

$$F_w^0 = \left(F_m - \frac{1}{2} m_1 g\right) \tan\theta \tag{3}$$

All of the parameters on the right-hand side of eq 3 are measurable using a surface tensiometer and a digital camera, and thus the driving force of the stationary boat F_w^0 can be obtained. The validity of this method was evaluated using the magnetic force (see Figure S2 of the Supporting Information).

THEORETICAL BACKGROUND

Mathematical Model for Self-Motion. A camphor boat spontaneously moves on the surface of water (Figure 2a). The self-motion of a camphor boat is thought to originate from the surface tension difference between the front and the back of the boat. When a camphor disk is attached at one side of the boat, surface tension around the camphor disk decreases while surface tension on the other side of the boat remains high because the plastic plate prevents the camphor molecules from spreading. Thus, the boat is pulled toward the opposite side to the camphor-attached edge (Figure 2b). Namely, the driving force of the self-propelled camphor boat is generated by the camphor molecular layer on the surface.

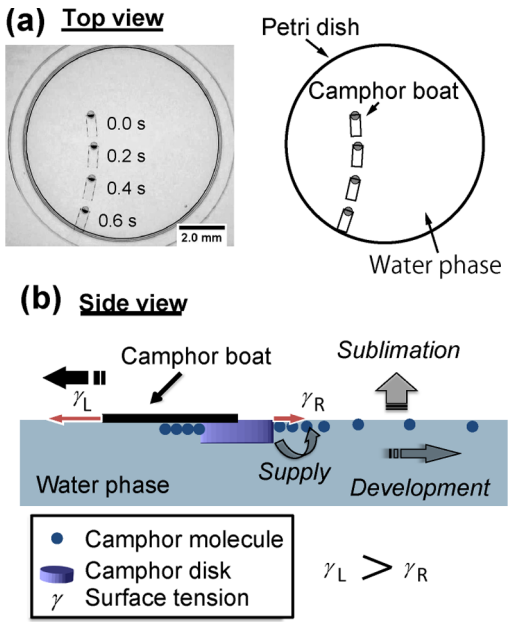

Figure 2. (a) A superimposed image of the self-motion of a camphor boat (left) and its illustration (right). The time interval is 0.2 s. (b) Illustration of the mechanism of self-motion. Camphor molecules are supplied from a camphor disk to the water surface and form a molecular layer. The molecular layer decreases surface tension on the right-hand side of the boat, and the surface tension difference then drives the boat to the left.

A mathematical model representing the behavior of camphor motion is constructed by two differential equations, the Newtonian equation and the reaction−diffusion equation, as described below:[16]

Newtonian equation:

$$m\frac{d^2x_0}{dt^2} = -\mu\frac{dx_0}{dt} + F_w \tag{4}$$

$$F_w = w(\gamma_0 - \gamma(\Gamma(x_0, t))) \tag{5}$$

Reaction-diffusion equation:

$$\frac{\partial\Gamma(x, t)}{\partial t} = D\nabla^2\Gamma(x, t) - k\Gamma(x, t) + \alpha L^{-1}\delta(x - x_0) \tag{6}$$

where the notation for the symbols is listed in Table A1 of the Appendix.

Time Derivative of the Mean Surface Concentration. Assuming the expansion of camphor molecules is sufficiently fast for the spatial gradient to be neglected, and the water phase is so large that the increase in the bulk concentration can be ignored, an ordinary differential equation for mean surface concentration of camphor $\Gamma(t)$ can be described as follows (see the Supporting Information):

$$\frac{d\Gamma(t)}{dt} = -k\Gamma(t) + \frac{n\alpha(p)}{A} \tag{7}$$

where n is the number of camphor boats placed on the water, $\alpha(p)$ is the supply rate of camphor molecules from the disk to the surface, and A is the surface area of the water phase. Supply rate $\alpha(p)$ is controlled by the attachment position p and is basically a function of the length of the perimeter bordering the water surface (L), which is $\pi\phi/2$ for p = 1.5 mm. The function of $\Gamma(t)$ can be obtained by solving eq 7 as follows:

$$\Gamma(t) = \frac{n\alpha(p)}{kA}[1 - \exp(-kt)] \tag{8}$$

For an ideal (usually dilute) solution of a single component surfactant, which is neither micellar nor an electrolyte, surface concentration is defined by the Gibbs adsorption isotherm as described below:[20]

$$\Gamma = -\frac{c}{RT}\left(\frac{\partial\gamma}{\partial c}\right) \tag{9}$$

where R is the gas constant (8.31 J mol^{-1} K^{-1}), T is absolute temperature (297 ± 1 K in our experiments), γ is surface tension, and c is bulk concentration. Using the Gibbs adsorption equation, one can derive the following equation for the Henry isotherm ($\Gamma = K_H c$) at the air/water interface:

$$\Pi = K_H RTc = RT\Gamma \tag{10}$$

where Π ($= \gamma_0 - \gamma$) is surface pressure. This relationship can be verified using the data for surface tension γ plotted as a function of camphor concentration c in the low concentration region (c

dx.doi.org/10.1021/la501628d | Langmuir 2014, 30, 8101−8108

< 2 mM, see Figure S3a in the Supporting Information) and surface concentration Γ against bulk concentration c (c < 1 mM, see Figure S3b of the Supporting Information). In this case, the Henry isotherm coefficient K_H was 2.42 μm. Using eq 10, eq 8 can be rewritten for surface pressure as follows:

$$\Pi(t) = \frac{n\alpha(p)RT}{kA}[1 - \exp(-kt)] \tag{11}$$

This equation, which can be applied to a large water phase system, indicates that the surface pressure rapidly increases at the initial stage and then reaches an equilibrium value, $n\alpha(p)RT/kA$.

Driving Force of a Camphor Boat. Here, a self-propelled camphor boat moving with a constant speed v_0 on a straight trajectory is considered. On a moving-coordinate system, the concentration profile behind the boat can be described in a steady state by the following (see the Supporting Information):

$$\Pi(x') = RT\Gamma(x') = \frac{RT\alpha(p)}{L\sqrt{v_0^2 + 4kD}} \exp\left[-\frac{\sqrt{v_0^2 + 4kD} - v_0}{2D}|x' - x_0'|\right] \tag{12}$$

Driving force F_w is obtained by $w\Pi(x')$. Assuming that w is comparable to the perimeter length (L) and that the surface pressure at the edge of the disk $\Pi(x_0')$ is a dominant contributor to the driving force, the driving force of the moving boat can be described as follows:

$$F_w = \frac{RT\alpha(p)}{\sqrt{v_0^2 + 4kD}} \tag{13}$$

This driving force balances with friction force under the mechanical steady-state condition. Thus, the following force balance is obtained:

$$F_w = \mu v_0 \tag{14}$$

Therefore, supply rate can be estimated using the following equation:

$$RT\alpha(p) = \mu v_0\sqrt{v_0^2 + 4kD} \tag{15}$$

On the other hand, from eq 13, the driving force F_w^0 of a stationary boat (v_0 = 0 mm s^{-1}), which can be measured using the direct mechanical measurement, is described as follows:

$$F_w^0 = \frac{RT\alpha(p)}{\sqrt{4kD}} \tag{16}$$

From eqs 15 and 16, the relationship between the equilibrium speed v_0 and the driving force F_w^0 can be described as follows:

$$F_w^0 = \mu v_0\sqrt{\frac{v_0^2}{4kD} + 1} \tag{17}$$

RESULTS

The time sequence of surface pressure was measured using the round boats moving over the entire surface of the water (Figure 1a). After floating the camphor boats (t = 0), surface pressure initially increased with time and then reached an equilibrium value (Figure 3a). To analyze the time series of surface pressure, the equilibrium surface pressure Π_e was determined as the average value after reaching the plateau and, consequently, the values for $\ln(1-\Pi/\Pi_e)$ were plotted as a function of time t (Figure 3b). In accordance with eq 11, the value of k can be determined from the slope of this plot and its value was (1.8 ± 0.4) × 10^{-2} s^{-1}. It should be noted that this value was nearly independent of the surface area of the water phase A (Figure 3c).

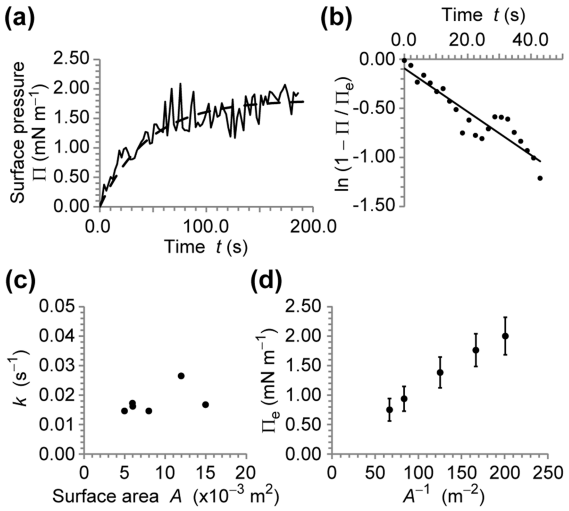

Figure 3. (a) Time series of the surface pressure (surface area of 50 cm^2). The dashed line indicates the fitted curve based on eq 11. (b) Single logarithmic plot of $(1-\Pi/\Pi_e)$ for the data shown in (a). The solid line is a linear fitted curve. (c) Characteristic time for the relaxation process (k). The value of k was nearly independent of the surface area. (d) Equilibrium surface pressure (Π_e) as a function of the inverse of the surface area (A^{-1}). The error bars indicate the standard deviation of the time series of the surface pressure after reaching the plateau.

The equilibrium value of Π_e corresponds to the coefficient of the right-hand side of eq 11. Thus, the slope of the plot of Π_e against A^{-1} (Figure 3d) corresponds to $n\alpha RTk^{-1}$ and was found to be (1.1 ± 0.1) × 10^{-5}. Using k = (1.8 ± 0.4) × 10^{-2} s^{-1} and the number of boats n = 5, the value for $RT\alpha$ was found to be (3.7 ± 1.0) × 10^{-8} J s^{-1}, which is the chemical energy supplied by a camphor boat in a unit of time. Therefore, supply rate α was (1.5 ± 0.4) × 10^{-11} mol s^{-1} for a boat with half of the camphor disk projected over water (p = 1.5 mm).

Three supply rates (supply to the water phase, to the air phase, and to the water surface) were determined by measuring the weight loss of camphor disks. First, the supply rate to the water phase (α_w) was evaluated from the slope of the time series of the weight loss (Figure 4a) and found to be (1.36 ± 0.04) × 10^{-6} g s^{-1}. Next, the weight loss of the camphor disk to the air phase was observed to increase linearly with time (Figure 4b), and the supply rate to the air phase (α_a) was determined to be (3.0 ± 0.3) × 10^{-7} g s^{-1}, which was the result of the sublimation rate from one side of the disk. Finally, the weight loss of a camphor disk moving on water (α_i) increased linearly with time up to 1000 s (Figure 4c). The slope was (1.70 ± 0.03) × 10^{-6} g s^{-1}. Using the molecular weight of camphor as 152, α_w, α_a, and α_i were calculated as (9.0 ± 0.2) × 10^{-9} mol s^{-1}, (2.0 ± 0.2) × 10^{-9} mol s^{-1}, and (11.2 ± 0.2) × 10^{-9} mol s^{-1}, respectively. α_i corresponds to $\alpha_a + \alpha + \alpha_w/2$ because one side of the camphor disk was exposed to the air phase and the other side was exposed to the water phase. Here, the second term corresponds to twice of α(1.5) because the

dx.doi.org/10.1021/la501628d | Langmuir 2014, 30, 8101−8108

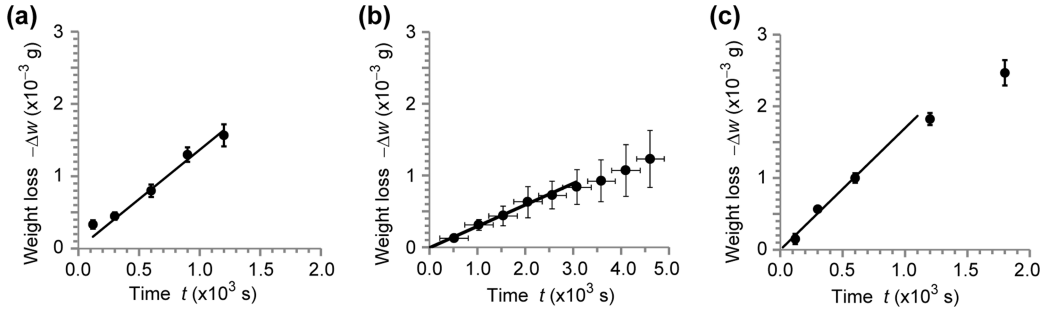

Figure 4. Time series for weight loss of a camphor disk (a) dipped in water while stirring, (b) placed in the air phase, and (c) moving on water. The error bars indicate standard deviation.

perimeter length of the disk was estimated to be twice that of the camphor boat (p = 1.5). Thus, the value of $\alpha(1.5)$ would be obtained by half of $(\alpha_i - \alpha_w/2 - \alpha_a)$. On the other hand, the value of the supply rate to the water surface $\alpha(1.5)$ was estimated as 1.5×10^{-11} mol s^{-1} from the data obtained for the surface pressure (Figure 3). This value was smaller than the error range for the values of the supply rates to the water phase and to the air phase. Therefore, the weight loss method was appropriate for determining the supply rates α_a and α_w but was not suitable for estimating the supply rate to the water surface $\alpha(p)$.

The profile of the camphor concentration on the surface of the water is determined by the competition between supply rate and spreading speed. The expansion of the camphor molecular layer can be visualized using particles. Therefore, the circular film of camphor molecules was obtained, and the time series of its radius was measured (Figure 5). The expansion behavior

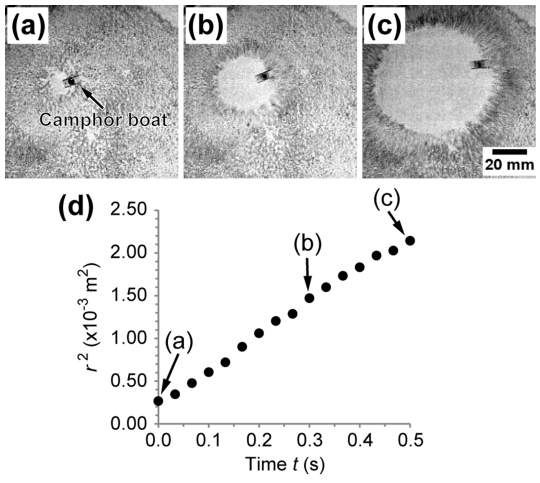

Figure 5. Expansion of the camphor molecular layer. (a–c) Snapshots indicating the behavior of the camphor layer visualized using particles dispersed on the water surface. The white region indicates the camphor layer. (d) Time series of the square of the radius of the camphor layer.

was similar to the diffusion process, although its speed was much faster.[21] This behavior is probably caused by Marangoni flow.[22−24] Here, the effective diffusion coefficient D was estimated as $(3.94 \pm 0.10) \times 10^{-3}$ m^2 s^{-1}.

The friction coefficient of the rectangular-shaped boat can be calculated from the relaxation process. For a boat with initial speed $v(0)$ and no driving force, the speed v exponentially decreases with time as follows:

$$v(t) = v(0)\exp\left(-\frac{\mu}{m}t\right) \tag{19}$$

where μ is the frictional coefficient and m is the mass of the boat (20 mg). Therefore, to estimate the value of the frictional coefficient of the boat, the time series of the speed for the intermittent motion was analyzed for the boat that exhibited relaxation-like motion after rapid acceleration (Figure 6). The

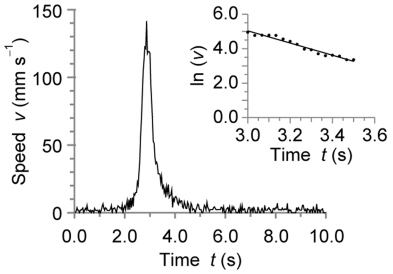

Figure 6. Profile of the speed of a camphor boat. After t = 3.0 s, the profile showed a relaxation-like process. The inset is a single logarithmic plot of $v(t)$ from t = 3.0−3.5 s.

slope of the single logarithmic plot of v corresponds to $-\mu/m$, which was found to be -3.5 ± 0.3 s^{-1} (Figure 6, inset). Thus, the frictional coefficient was calculated to be $(7.0 \pm 0.7) \times 10^{-5}$ N m^{-1} s.

Driving force for the rectangular-shaped boat was estimated from F_m and θ (Figure 1c). Here, seven boats were prepared with different driving forces. The variation in driving force was achieved by varying the attachment position of the camphor disk (p: 0.0−1.5 mm). Equilibrium speed v_0 for self-motion and the stationary driving force F_w^0 were measured for each boat (Table 1 and Figure 7). The plot in Figure 7 indicates that driving force was positively correlated with the speed of self-motion, and these experimental data were also in good agreement with the calculated results obtained using eq 17

Table 1. Experimentally Determined Values for the Driving Force of the Stationary Camphor Boat

p (mm)	v_0 (mm s^{-1})	F_1 (μN)	$(180/\pi)\theta$ (deg)	F^0_W (μN)
1.5	66 ± 3	147	11.7	23.4
1.1	53 ± 3	186	4.0	10.7
1.0	61 ± 2	152 ± 7	10.8 ± 1.4	22.3 ± 1.6
0.5	58 ± 2	152 ± 14	9.4 ± 0.9	19.4 ± 2.2
0.4	41 ± 2	137	4.5	8.1
0.0	41 ± 2	125 ± 27	2.4 ± 0.6	3.6 ± 0.8
0.0	32 ± 4	137	1.6	2.8

dx.doi.org/10.1021/la501628d | Langmuir 2014, 30, 8101−8108

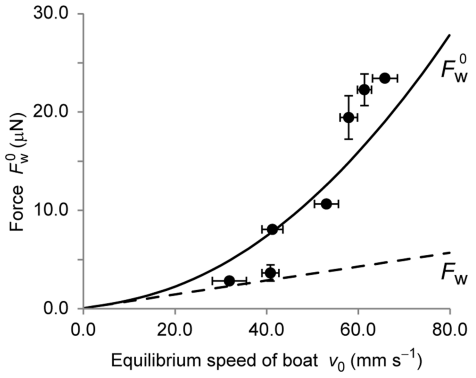

Figure 7. Relationship between driving force and the propelling speed of camphor boats with different attachment positions of the camphor disks. Error bars for the vertical axis indicate the standard deviation of repeat measurements for the same boat, while those for the horizontal axis indicate the standard deviation for the time series of the speed. The solid curve was obtained using eq 17 and the dashed line using eq 14.

(solid line in Fig. 7). The dashed line in Figure 7 indicates the driving force of the moving boat (F_w), which is obtained using eq 14. As the motion induced the expansion of the camphor profiles, the surface pressure around the stationary boat became larger than that of the moving one. This deviation is represented by the nonlinear term in eq 17. So, the driving forces (F_w and F_w^0) were proportional to the speed v_0 in the low-speed region [$v_0 \ll (4kD)^{1/2} \approx 10$ mm s^{-1} as the linear region], while F_w^0 became larger than the linear value in the higher speed region. When p was 1.5 mm, the boat exhibited maximum speed (66 mm s^{-1}); the driving force working on the moving boat should be $F_w = 4.2$ μN.

DISCUSSION

The various parameters estimated using two types of camphor boats (i.e., round-shaped and rectangular-shaped boats) are presented in Table 2. Parameters k and D represent properties of the camphor molecular layer on the water surface and thus

Table 2. Parameter Set for the Surface Behavior of Camphor Molecules and the Self-Propelled Camphor Boat

	notation	value
(reaction−diffusion equation)		
relaxation rate (sum of sublimation rate and dissolution rate of the molecules on water surface)	k	$(1.8 \pm 0.4) \times 10^{-2}$ s^{-1}
effective diffusion coefficient	D	$(3.94 \pm 0.10) \times 10^{-3}$ m^2 s^{-1}
supply rate of camphor molecules from the camphor disk to the water surface (the attached position p = 1.5 mm)	α (1.5)	$(1.5–12.5) \times 10^{-11}$ mol s^{-1}
(Newtonian equation)		
friction coefficient	μ	$(7.0 \pm 0.7) \times 10^{-5}$ N m^{-1} s
driving force of the moving camphor boat (v_0 = 66 mm s^{-1})	F_w	4.2×10^{-6} N
surface tension difference between the front and the back of the boat	$\Delta\gamma$	1.1×10^{-3} N m^{-1}
(others)		
supply rate to the water phase	α_w	$(9.0 \pm 0.2) \times 10^{-9}$ mol s^{-1}
supply rate to the air phase (one side of the disk is exposed)	α_a	$(2.0 \pm 0.2) \times 10^{-9}$ mol s^{-1}

can be used for a wide range of situations independent of the shape of the camphor boat. The supply rate of camphor molecules from the disk to the water surface (α) may be proportional to the length of the contact line between the camphor disk and the water surface (L). Thus, the parameter α listed in Table 2 should be applicable for any camphor boat independent of its shape as long as half of the camphor disk protrudes from the edge of boat (p = 1.5 mm), even though the value for α(1.5) had a wide range (almost one order, see below). On the other hand, the friction coefficient (μ) strongly depends on the properties of the camphor boat, such as its size and shape. Therefore, the value of this parameter is only suitable for the rectangular-shaped boat used in this study.

On the basis of eq 15, the value of the supply rate for each boat can be calculated from the equilibrium speed of the boat (v_0). The boat with one-half of the camphor disk protrudes from the edge moved at 66 mm s^{-1}. Thus, the supply rate α(1.5) was calculated to be 1.25×10^{-10} mol s^{-1}. This value is almost one order of magnitude greater than that obtained from the analysis of the time series of surface pressure. In principle, the flow around the camphor disks induced by the surface tension gradient (i.e., Marangoni flow), which may influence the motion of the camphor boat and the surface concentration profile of the camphor disk,[22−24] must be considered. This effect would change the force balance and cause inconsistency in the supply rate. Furthermore, to derive eq 7, it was assumed that the camphor concentration was spatially homogeneous on the surface. However, the concentration close to the camphor disk may be higher than the concentration farther away; because surface tension was measured at a distant point from the disk, if this inhomogeneity is not negligible, the estimated value of the surface pressure around the boat would be lower than the true value. As a result, the value of α estimated using the surface pressure may be smaller than the actual value.

As can be seen in Figure 7, the directly measured driving forces were consistent with the values calculated using eq 17. This agreement indicates that the values of the frictional coefficient (μ), effective diffusion coefficient (D), characteristic time (k), and driving forces (F_w^0) are consistent, and that eqs 13 and 14 are valid. Moreover, the estimation of the surface tension difference as 1.1 mN/m is comparable to that recently reported by Fujinami et al. in which surface tension difference between the front and the back of a camphor boat was estimated to 0.4−1.3 mN/m by directly measuring the surface tension using the quasi-elastic laser scattering method.[25] This evidence strongly support the validity of our method and observation results.

CONCLUSION

We measured the parameters for self-propelled camphor boats as listed in Table 2. Given the values of the friction coefficient, effective diffusion coefficient, and relaxation rate, the stationary driving force was estimated from the equilibrium speed via eq 17. The calculated results were in good agreement with the results obtained using the direct mechanical measurement (Figure 7). Therefore, the experimental and calculated data for the parameters listed in Table 2 were fairly consistent, except for the value of supply rate. We believe that this quantitative information will enable further investigation and application of both camphor and other self-propelled systems because the data can be quantitatively used to discuss the possibility of novel self-propelled systems based on surface chemistry. Furthermore, it was demonstrated that the mathematical

dx.doi.org/10.1021/la501628d | Langmuir 2014, 30, 8101−8108

models for these systems can be quantitatively verified. As a result, such quantitative approaches would achieve breakthrough innovations and the development of novel and smart self-propelled systems.

APPENDIX

Table A1. Notation of the symbols

ϕ	diameter of the camphor disk (= 3×10^{-3})	[m]
w	width of the rectangular-shaped boat (= 4×10^{-3})	[m]
p	attached position of the camphor disk	[m]
α_a	supply rate of camphor molecules to the air phase	[mol s^{-1}]
α_w	supply rate of camphor molecules to the water phase	[mol s^{-1}]
α_i	supply rate of camphor molecules to the water surface	[mol s^{-1}]
F_m	force working on the detector	[N]
F_w^0	driving force of the stationary camphor boat	[N]
θ	angle of the tilt of the Pt wire	[rad]
m_1	weight of the Pt wire (= 7×10^{-6})	[kg]
l	length of the Pt wire (= 0.1)	[m]
m	mass of the camphor boat (= 20×10^{-6})	[kg]
x_0	position at the edge of the camphor disk	[m]
μ	friction coefficient	[N m^{-1} s]
F_w	driving force of the moving camphor boat	[N]
γ	surface tension	[N m^{-1}]
γ_0	surface tension of pure water	[N m^{-1}]
Γ	surface camphor concentration	[mol m^{-2}]
D	effective diffusion coefficient	[m^2 s^{-1}]
k	sum of k_s and k_d	[s^{-1}]
k_s	sublimation rate from the water surface	[s^{-1}]
k_d	dissolution rate from the water surface	[s^{-1}]
L	length of the contact line between the camphor disk and the water surface	[m]
n	number of camphor boats placed on the water surface	[boat]
$\alpha(p)$	supply rate of camphor molecules from the disk to the water surface depending on the attached position p of the camphor disk to the plastic plate	[mol s^{-1}]
A	surface area of the water phase.	[m^2]
R	gas constant (= 8.31)	[J mol^{-1} K^{-1}]
T	absolute temperature (= 297 ± 1)	[K]
c	camphor concentration in the bulk	[mol m^{-3}]
Π	surface pressure (= $\gamma_0 - \gamma$)	[N m^{-1}]
K_H	Henry isotherm coefficient	[m]
v_0	speed of the camphor boat in a steady state	[m s^{-1}]
x_0'	position at the edge of the camphor disk on the moving-coordinate system	[m]

ASSOCIATED CONTENT

Supporting Information

(i) A second measurement of the weight loss of the camphor disk, (ii) the calibration curve for the direct mechanical method, (iii) data for the surface tension and surface concentration as a function of the bulk camphor concentration, (iv) derivation of the ordinary differential equation for the surface concentration, and (v) derivation of eq 12 for the surface concentration profile behind a moving camphor boat. This material is available free of charge via the Internet at http://pubs.acs.org

.

AUTHOR INFORMATION

Corresponding Author

*E-mail: suematsu@meiji.ac.jp.

Author Contributions

The manuscript was written through contributions of all authors. All authors have given approval to the final version of the manuscript.

Notes

The authors declare no competing financial interest.

ACKNOWLEDGMENTS

The authors would like to thank Prof. Hiraku Nishimori (Hiroshima University, Japan) and Prof. Kohta Ikeda (Meiji University, Japan) for their helpful discussions. This work was supported in part by Grants-in-aid for Young Scientists (B) to N.J.S. (Grant 23740299) and H.K. (Grant 24740256), a Grant-in-aid for Scientists (C) to S.N. (Grant 25410094), and a Grant-in-aid for Scientific Research on Innovative Areas "Fluctuation & Structure" to H.K. (Grant 25103008) from the Japan Society for the Promotion of Science (JSPS), the JSPS Core-to-Core Program "Nonequilibrium dynamics of soft matter and information" (H.K.), the Japan Science and Technology Agency Precursory Research for Embryonic Science and Technology (PRESTO) program (H.K.), the Sekisui Chemical Grant Program for Research on Manufacturing Based on Innovations Inspired by Nature (S.N.), Research Project Grant (B) by Institute of Science and Technology Meiji University (N.J.S.), and the Meiji University Global COE Program "Formation and Development of Mathematical Sciences Based on Modeling and Analysis" from the Ministry of Education, Culture, Sports, Science, and Technology (MEXT), Japan.

REFERENCES

(1) Hilner, E.; Zakharov, A. A.; Schulte, K.; Kratzer, P.; Andersen, J. N.; Lundgren, E.; Mikkelsen, A. Ordering of the Nanoscale Step Morphology As a Mechanism for Droplet Self-Propulsion. *Nano Lett.* **2009**, *9*, 2710−2714.

(2) Shioi, A.; Ban, T.; Morimune, Y. Autonomously Moving Colloidal Objects that Resemble Living Matter. *Entropy* **2010**, *12*, 2308−2332.

(3) Wang, J. *Nanomachines*; Wiley-VCH: Germany, 2013.

(4) Ebbens, J. S.; Howse, R. J. In Pursuit of Propulsion at the Nanoscale. *Soft Matter* **2010**, *6*, 726−738.

(5) Bánsági, T., Jr.; Wrobel, M. M.; Scott, S. K.; Taylor, A. F. Motion and Interaction of Aspirin Crystals at Aqueous-Air Interfaces. *J. Phys. Chem. B* **2013**, *117*, 13572−13577.

(6) Sumino, Y.; Magome, N.; Hamada, T.; Yoshikawa, K. Self-Running Droplet: Emergence of Regular Motion from Nonequilibrium Noise. *Phys. Rev. Lett.* **2005**, *94*, 068301.

(7) Sharma, R.; Chang, S. T.; Velev, O. D. Gel-Based Self-Propelling Particles Get Programmed to Dance. *Langmuir* **2012**, *28*, 10128−10135.

(8) Jin, H.; Marmur, A.; Ikkala, O.; Ras, R. H. A. Vapour-Driven Marangoni Propulsion: Continuous, Prolonged and Tunable Motion. *Chem. Sci.* **2012**, *3*, 2526−2529.

(9) Ban, T.; Yamagami, T.; Nakata, H.; Okano, Y. pH-Dependent Motion of Self-Propelled Droplets due to Marangoni Effect at Neutral pH. *Langmuir* **2013**, *29*, 2554−2561.

(10) Banno, T.; Kuroha, R.; Toyota, T. pH-Sensitive Self-Propelled Motion of Oil Droplets in the Presence of Cationic Surfactants Containing Hydrolyzable Ester Linkages. *Langmuir* **2012**, *28*, 1190−1195.
(11) Thutupalli, S.; Seemann, R.; Herminghaus, S. Swarming Behavior of Simple Model Squirmers. *New J. Phys.* **2011**, *13*, 073021.
(12) Nakata, S.; Iguchi, Y.; Ose, S.; Kuboyama, M.; Ishii, T.; Yoshikawa, K. Self-Rotation of a Camphor Scraping on Water: New Insight into the Old Problem. *Langmuir* **1997**, *13*, 4454−4458.
(13) Mikhailov, A. S.; Calenbuhr, V. *From Cells to Societies; Models of Complex Coherent Action*; Springer: Germany, 2006.
(14) Nagayama, M.; Nakata, S.; Doi, Y.; Hayashima, Y. A Theoretical and Experimental Study on the Unidirectional Motion of a Camphor Disk. *Physica D* **2004**, *194*, 151−165.
(15) Hayashima, Y.; Nagayama, M.; Doi, Y.; Nakata, S.; Kimura, M.; Iida, M. Self-Motion of a Camphoric Acid Boat Sensitive to the Chemical Environment. *Phys. Chem. Chem. Phys.* **2002**, *4*, 1386−1392.
(16) Suematsu, N. J.; Nakata, S.; Awazu, A.; Nishimori, H. Collective Behavior of Inanimate Boats. *Phys. Rev. E* **2010**, *81*, 056210.
(17) Soh, S.; Branicki, M.; Grzybowski, B. A. Swarming in Shallow Water. *J. Phys. Chem. Lett.* **2011**, *2*, 770−774.
(18) Tomlinson, C. On the Motion of Camphor on the Surface of Water. *Proc. R. Soc. London* **1862**, *11*, 575−577.
(19) Suematsu, N. J.; Ikura, Y.; Nagayama, M.; Kitahata, H.; Kawagishi, N.; Murakami, M.; Nakata, S. Mode-Switching of the Self-Motion of a Camphor Boat Depending on the Diffusion Distance of Camphor Molecules. *J. Phys. Chem. C* **2010**, *114*, 9876−9882.
(20) Chang, C.-H.; Franses, E. I. Adsorption Dynamics of Surfactants at the Air/Water Interface: A Critical Review of Mathematical Models, Data, and Mechanisms. *Colloids Surf., A* **1995**, *100*, 1−45.
(21) Delgado, J. M. P. Q. Molecular Diffusion Coefficients of Organic Compounds in Water at Different Temperature. *J. Phase Equilib. Diffus.* **2007**, *28*, 427−432.
(22) Kitahata, H.; Hiromatsu, S.; Doi, Y.; Nakata, S.; Islam, M. R. Self-motion of a Camphor Disk Coupled with Convection. *Phys. Chem. Chem. Phys.* **2004**, *6*, 2409−2414.
(23) Kovalchuk, V. I.; Kamusewitz, H.; Vollhardt, D.; Kovalchuk, N. M. Auto-Oscillation of Surface Tension. *Phys. Rev. E* **1999**, *60*, 2029−2036.
(24) Kovalchuk, N. M.; Kovalchuk, V. I.; Vollhardt, D. Numerical Study of the Marangoni Instability Resulting in Surface Tension Auto-Oscillations: General Regularities of the System Evolution. *Phys. Rev. E* **2001**, *63*, 031604.
(25) Karasawa, Y.; Oshima, S.; Nomoto, T.; Toyota, T.; Fujinami, M. Simultaneous Measurement of Surface Tension and Its Gradient around a Moving Camphor Boat on a Water Surface. *Chem. Lett.*, in press.